Available on the CERN CDS information server **CMS PAS HIG-12-007**

CMS Physics Analysis Summary

Contact: cms-pag-conveners-higgs@cern.ch 2012/03/07

Search for Neutral Higgs Bosons Decaying into Tau Leptons in the Di-Muon Channel in pp Collisions at 7 TeV

The CMS Collaboration

Abstract

A search for neutral Higgs boson decays into tau lepton pairs in a final state characterized by two muons and missing transverse energy is presented. The study is based on a data set corresponding to an integrated luminosity of 4.5 fb^{-1} collected with the CMS detector at the LHC at a center-of-mass energy of 7 TeV. The search is performed in the context of the Standard Model (SM) and the Minimal Supersymmetric Standard Model (MSSM). Included are the cases where the Higgs boson is produced with two forward jets in the vector boson fusion process (SM search), or with a high-p_{T} hadronic jet (SM search), or in association with a b-quark jet (MSSM search). No significant excess of events over background expectations is observed and 95% CL upper limits on the cross section of the Higgs boson production in the SM and on model parameters in the MSSM scenarios are presented.

1 Introduction

The standard model (SM) has been extremely successful in describing a wide range of phenomena in particle physics, and has survived some four decades of experimental testing. The search is underway at the Large Hadron Collider (LHC) for the only remaining undiscovered fundamental particle predicted by the SM, the Higgs boson [1–6].

However, the Higgs boson in the SM suffers from quadratically divergent self-energy corrections at high energies [7]. Numerous extensions to the SM have been proposed to address these divergences. One such model is supersymmetry [8], a symmetry between fundamental bosons and fermions, which leads to a cancellation of divergences present in the SM. The minimal supersymmetric extension to the standard model (MSSM) requires the presence of two Higgs doublets. This leads to a more complicated scalar sector, with five massive Higgs bosons: a light neutral CP-even state (h), two charged states ($H^{\pm}$), a heavy neutral CP-even state (H) and a neutral CP-odd state (A).

The masses of MSSM Higgs bosons are defined, up to radiative corrections, by two parameters, usually taken to be the mass of the CP-odd state, m_A, and the ratio of the vacuum expectation values of the two Higgs doublets, $\tan\beta$. The mass relations among the neutral MSSM Higgs bosons are such that if $m_A \lesssim 130$ GeV, at large values of the parameter $\tan\beta$, the masses of the h and A are nearly degenerate, while that of the H is approximately 130 GeV. If $m_A \gtrsim 130$ GeV, then the masses of the A and H are nearly degenerate, while that of the h remains near 130 GeV. The precise value of the crossover point depends predominantly on the nature of the mass mixing in the top-squark states.

This document reports a search for the SM and the neutral MSSM Higgs bosons in pp collisions at $\sqrt{s} = 7$ TeV at the LHC, recorded by the Compact Muon Solenoid (CMS) experiment. The analysis uses the decays of neutral Higgs bosons into tau lepton pairs with subsequent decay of each tau lepton into a muon and two neutrinos, denoted as $\tau_\mu\tau_\mu$. This study complements the searches for neutral Higgs boson decays to $\tau\tau$ performed by the CMS Collaboration on the same data set [9] in other three independent τ pair final states: $\tau_e\tau_h$, $\tau_\mu\tau_h$ and $\tau_e\tau_\mu$, where τ_e denotes a tau lepton decaying into an electron and two neutrinos, and τ_h a hadronically decaying τ. Those searches are similar to the searches performed by the ATLAS experiment [10] and at the Tevatron [11] and are complementary to the MSSM Higgs search at LEP [12].

In the case of SM Higgs boson production at the LHC (Figure 1), the gluon fusion process has the largest cross section. However, the background from Drell-Yan production of muon pairs ($Z/\gamma^* \to \mu\mu$) and tau pairs ($Z \to \tau\tau$) overwhelms the expected Higgs boson signal in the mass region of interest. The results of studies of two processes are presented in this document for which these backgrounds are suppressed, namely the vector boson fusion (VBF) production of Higgs bosons, and the production of a highly boosted Higgs boson in association with a high-p_T hadronic jet. The VBF channel, with its distinct topology of two jets in the forward and backward hemisphere with a large separation in rapidity, has a better sensitivity due to the greatly reduced background from $Z/\gamma^* \to \mu\mu, \tau\tau$. Requiring a high-$p_T$ jet, recoiling against the Higgs boson, greatly reduces the background from $Z/\gamma^* \to \mu\mu, \tau\tau$ and improves the resolution of the tau-pair invariant mass.

In the MSSM scenario (Figure 2), two main production processes contribute to $pp \to \phi + X$, where $\phi = h, H$, or A: gluon fusion through a b quark loop and direct $b\bar{b}$ annihilation from b partons in the colliding protons. In the latter case, there is a significant probability that a b-quark jet is produced centrally in association with the Higgs boson. The subsample in which there is a b-tagged jet has increased sensitivity for the MSSM Higgs boson search due to the

smaller relative contribution from inclusive Z boson production.

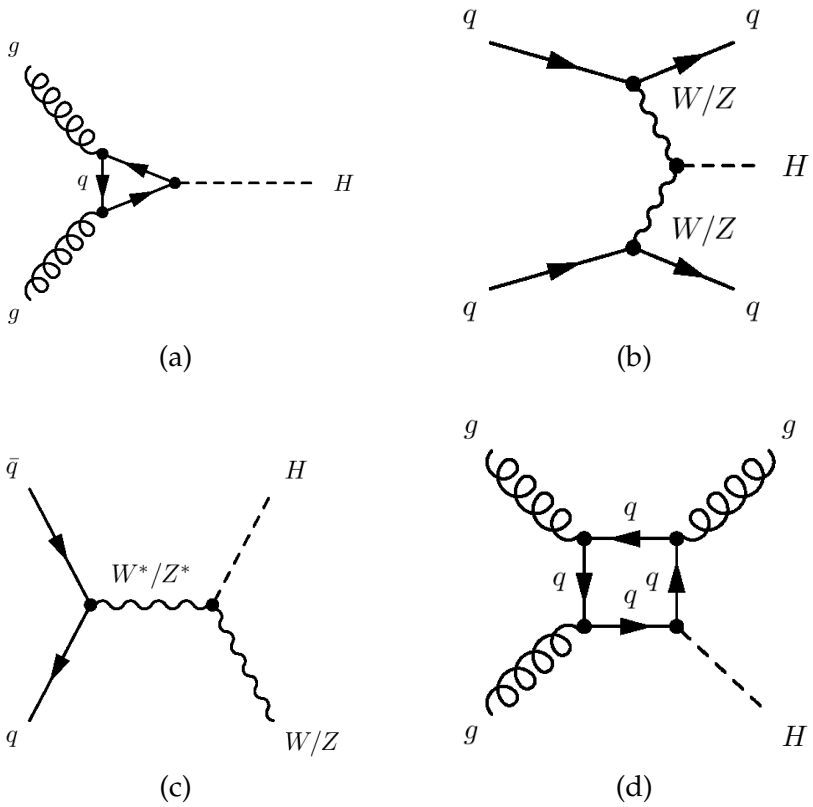

Figure 1: Feynman diagrams for the dominating SM Higgs boson production modes at the LHC: (a) gluon fusion; (b) vector boson fusion; (c) and (d): production of a boosted Higgs boson in association with a high-p_{T} hadronic jet.

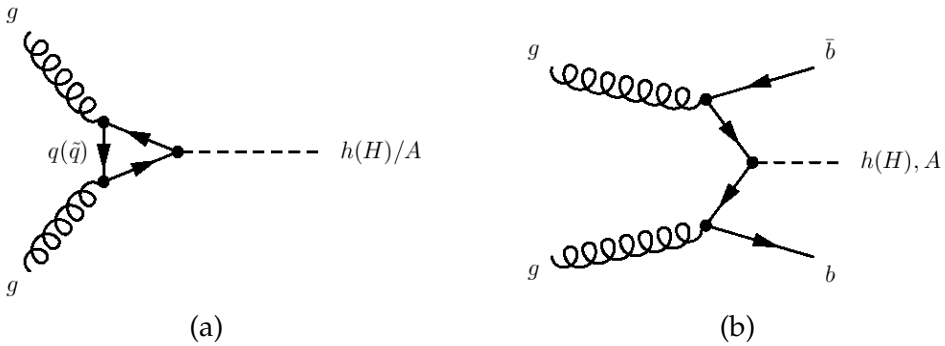

Figure 2: Feynman diagrams for the dominating MSSM Higgs boson production modes at the LHC: (a) gluon fusion through a b quark loop; (b) direct $\mathrm{b\bar{b}}$ annihilation from b partons in the colliding protons.

2 CMS Detector and Data

The central feature of the CMS apparatus [13] is a superconducting solenoid, of 6 m internal diameter, providing a field of 3.8 T. The key components of the detector include a silicon pixel and strip tracker, which is used to measure the momenta of charged particles. The tracker, which

covers the pseudorapidity range $|\eta| < 2.5$, is surrounded by a crystal electromagnetic calorimeter and a brass-scintillator hadronic calorimeter. These calorimeters extend to a pseudorapidity range of $|\eta| < 3.0$. A quartz fiber Cherenkov forward detector extends the calorimetric coverage to $|\eta| < 5.0$. The outermost component of the CMS detector is the muon system consisting of gas detectors placed in the steel return yoke to measure the momenta and angles of muons.

The data set used in this analysis, collected in the year 2011 in pp collisions at $\sqrt{s} = 7$ TeV, amounts to an integrated luminosity of 4.5 fb^{-1}.

The Monte-Carlo (MC) event generators PYTHIA [14] and POWHEG [15] are used to model the MSSM and SM Higgs boson signals. Di-boson and QCD multijet backgrounds are simulated by PYTHIA. Inclusive Z and W boson production and $\mathrm{t\bar{t}}$ events are modeled with MADGRAPH. The TAUOLA [16] package is used for tau decays in all cases. Additional next-to-next-to-leading order (NNLO) k-factors for the Higgs boson p_T spectrum from FEHIPRO [17, 18] are applied to all simulated events with Higgs bosons produced through gluon fusion.

3 Trigger and Event Selection

For roughly the first quarter of the data, a single isolated muon is required at the trigger level with a transverse-momentum (p_T) threshold of 17 GeV/c, while for the rest of the data, a double muon trigger with thresholds of 8 GeV/c and 13 GeV/c is used [19].

The analysis uses a particle-flow technique [20, 21], in which the information from all CMS sub-detectors is combined to identify and reconstruct individual particles in the event, namely muons, electrons, photons, and charged and neutral hadrons. The list of these particles is used as input to the jet, tau, and missing transverse energy ($\not\!\!E_\mathrm{T}$) reconstruction. Hadronic jets are reconstructed using the anti-k_T jet algorithm [22] with a resolution parameter set to $\Delta R = 0.5$.

In the year 2011, the average number of pp interactions per LHC bunch crossing ("pile-up") was about ten. The simulated MC events are reweighted to represent the number of pile-up events in data. For each reconstructed collision vertex, the sum of the p_T^2 of all tracks associated to the vertex is computed. The vertex for which this quantity is the largest is assumed to correspond to the hard-scattering process, and is referred to as the primary vertex.

Events with at least one pair of oppositely charged muons are selected. The leading muon is required to have $p_\mathrm{T} > 20$ GeV/c and $|\eta| < 2.1$, where η denotes the pseudorapidity of the reconstructed muon. The sub-leading muon is required to have $p_\mathrm{T} > 10$ GeV/c and $|\eta| < 2.4$ (2.1) for the samples triggered by the single (double) muon trigger.

Since muons stemming from the decay of tau-leptons are isolated from hadronic activity, each of the muons is required to be isolated from the rest of the event activity. A relative isolation variable is constructed from the sum of the transverse momenta p_T of all reconstructed charged particles contained within a cone $\Delta R < 0.4$ with respect to the direction of the muon three-momentum, excluding the contribution from the muon candidate itself.

Tau-leptons have a decay length exceeding one millimeter (for tau-lepton momenta larger than 20 GeV/c), which causes muon tracks from the decay of tau-leptons to be displaced with respect to each other. This tau decay length information is accounted for by constructing the inter-muon distance of closest approach (DCA) significance. The latter is defined as the three-dimensional DCA between two tracks, divided by the resolution on this quantity.

Another characteristc signature of the studied process is the missing transverse energy $\not\!\!E_\mathrm{T}$ apportioned to the unknown amount of energy and momentum carried away by the neutrinos

escaping the detection. In the simulated samples, the simulation of the $\not{E}_T$ distribution is improved by applying corrections to the resolution of the hadron recoil transverse momentum projected onto the direction parallel and perpendicular to the Z, W or Higgs boson transverse momenta in the corresponding simulated MC samples. The resolution functions are extracted from observed $Z/\gamma^* \to \mu\mu$ events for different ranges of the Z boson p_T and jet multiplicity bins. These resolution functions are then used to correct the MC simulation in order to match the experimental data.

The analysis in the MSSM case employs an algorithm [23] that identifies b-quark jets based on the impact parameter of the tracks associated with the reconstructed jet.

In order to enhance the sensitivity of the search for Higgs bosons in both the SM and the MSSM, selected events are classified into several categories based on the number of selected jets and b-tagged jets.

For the SM search, three categories are defined, which are mutually exclusive:

- **The *VBF* category** requires at least two jets with $p_T > 30$ GeV/c, $|\eta_1 - \eta_2| > 4.0$ and $\eta_1 \cdot \eta_2 < 0$ (with η_1 the pseudorapidty of the leading jet and η_2 the pseudorapidity of the subleading jet), and a di-jet invariant mass $m_{12} > 400$ GeV/c^2, with no other jet with $p_T > 30$ GeV/c in the rapidity region between the two jets.
- **The *Boosted* category** requires at least one jet with $p_T > 150$ GeV/c.
- **The *0/1-Jet* category** requires at most one jet with $p_T > 30$ GeV/c, and, if such a jet is present, it must have $p_T < 150$ GeV/c.

For the MSSM search, two categories are defined, which are mutually exclusive:

- **The *B-Tag* category** contains events with at most one jet with $p_T > 30$ GeV/c (no b-tag requirement applied) and at least one b-tagged jet with $p_T > 20$ GeV/c.
- **The *Non B-Tag* category** contains events with at most one jet with $p_T > 30$ GeV/c (no b-tag requirement applied) and no b-tagged jet with $p_T > 20$ GeV/c.

A multi-variate analysis technique based on the likelihood ratio method [24] is employed, combining variables that discriminate the Higgs signal from the predominant $Z/\gamma^* \to \mu\mu$ and $Z \to \tau\tau$ background contributions into one likelihood discriminant. The variables used for the MSSM search and the SM search in the *0/1-Jet* category are:

1. The ratio of the transverse momentum of the muon-pair to the scalar sum of the two muon transverse momenta, $p_T(2\mu)/(p_T(\mu^+) + p_T(\mu^-))$.
2. The pseudorapidity of the muon-pair system, $\eta(2\mu)$.
3. The inter-muon DCA significance, $\log_{10}(\mathrm{DCASig}(2\mu))$.
4. The azimuthal angle between the direction of the positively charged muon three-momentum and the missing transverse energy, $\Delta\Phi(\mu^+, p_T^{\mathrm{miss}})$.
5. The validity of the collinear approximation (CA) [25], represented by a binary variable and assuming that the neutrinos from the tau decay are emitted predominantly along the direction of the three-momentum of the muon. The reconstruction of the tau pair yields a valid solution if it is possible to construct a vector pointing in the direction of the missing transverse energy. Otherwise the solution is denoted as invalid.

The distributions of these variables are shown in Figure 3 for data and MC samples, for a representative Higgs boson mass hypothesis of m_A =200 GeV/c^2 and $\tan\beta = 20$. In the case of the SM searches in the *VBF* (Figure 4) and *Boosted* (Figure 5) categories, variables 1. and 2. are not used, and the missing transverse energy is chosen instead.

An event is selected to be in a given event category if the individual likelihood discriminant exceeds a certain value. This threshold is optimized individually for each event category and for each tested Higgs boson mass hypothesis. The optimization exploits a log-likelihood ratio test estimator

$$\log Q = \sum_i (S_i - N_i \log(1 + S_i/B_i)). \tag{1}$$

The index of the sum runs over all bins of the distributions used for the statistical inference, S_i (B_i) is the number of expected signal (background) events and N_i is the number of observed events in bin i. The optimization of cut is performed by maximizing the quantity

$$\log Q_{(\mathrm{S+B})} - \log Q_{(\mathrm{B})}, \tag{2}$$

where $\log Q_{(\mathrm{S+B})}$ is the log-likelihood ratio expected from the "signal-plus-background" hypothesis (S+B),

$$\log Q_{(\mathrm{S+B})} = \sum_i (S_i - (S_i + B_i) \log(1 + S_i/B_i)), \tag{3}$$

and $\log Q_{(\mathrm{B})}$ is the log-likelihood ratio expected from the "background-only" hypothesis (B),

$$\log Q_{(\mathrm{B})} = \sum_i (S_i - B_i \log(1 + S_i/B_i)). \tag{4}$$

Table 1 lists the resulting Higgs boson signal efficiencies for the different event categories for a representatively chosen Higgs boson mass hypothesis $m_H = 120$ GeV/c^2 in the SM search and $m_A = 200$ GeV/c^2 in the MSSM search. In case of the SM search, the requirements on the likelihood discriminant L are $L > 0.9$ for the *Boosted* and *VBF* event categories and $L > 0.4$ for the *0/1-Jet* category. This requirement is independent of the probed Higgs boson mass. For an MSSM Higgs boson mass of $m_A = 200$ GeV/c^2, the requirement is $L > 0.6$ for the *Non B-Tag* and $L > 0.3$ for the *B-Tag* event category.

Table 1: Signal acceptances for a MSSM Higgs boson with $m_A = 200$ GeV/c^2 via gluon fusion ($gg \to \phi$) or $b\bar{b}$ annihilation ($gg \to b\bar{b}\phi$) and for a SM Higgs boson with $m_H = 120$ GeV/c^2 produced via gluon fusion ($gg \to H$), VBF ($qq \to qqH$) or associated production with W or Z bosons or top-quark pairs ($qq \to Ht\bar{t}/V$).

Signal Selection Efficiency $\times$ Acceptance ($\epsilon \times \mathcal{A}$), in percent

	Standard Model $m_H = 120$ GeV/c^2			MSSM $m_A = 200$ GeV/c^2	
Category	*0/1-Jet*	*Boosted*	*VBF*	*Non B-Tag*	*B-Tag*
$gg \to H$	6.16	0.23	<0.04	-	-
$qq \to qqH$	4.35	0.60	3.28	-	-
$qq \to t\bar{t}H/VH$	8.78	0.45	<0.02	-	-
$gg \to \phi$	-	-	-	8.58	0.33
$gg \to b\bar{b}\phi$	-	-	-	8.26	3.08

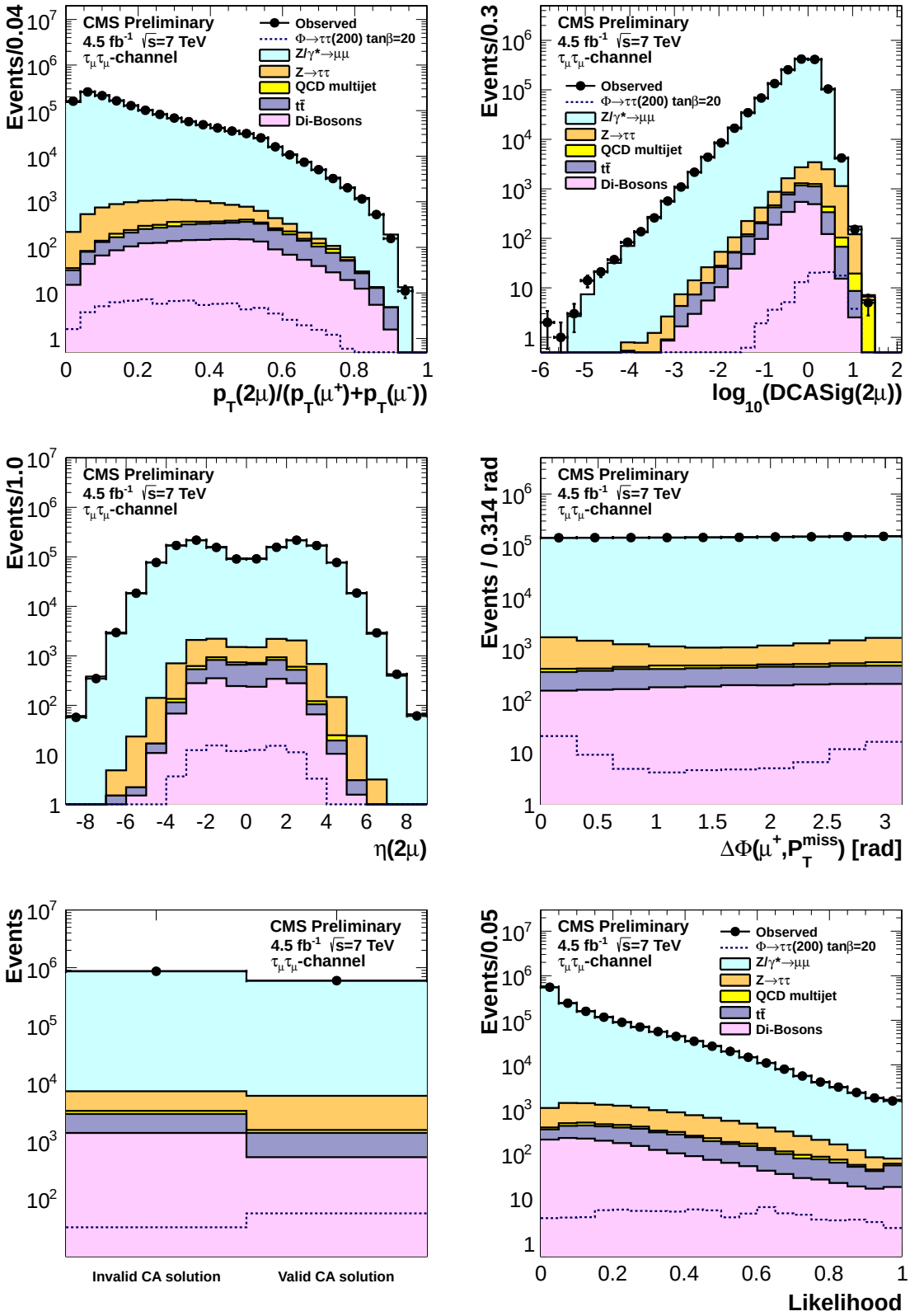

Figure 3: Distributions of discriminating variables used to construct the likelihood discriminant for the MSSM Higgs boson search and for the *0/1-Jet* category in the SM search. See text for the definition of the variables. 2011 data, represented by circles, are compared with the MC background samples, displayed as filled histograms. The $\phi \to \tau\tau$ signal expected for $m_A = 200\,\text{GeV}/c^2$ and $\tan\beta = 20$ is shown as dashed histogram.

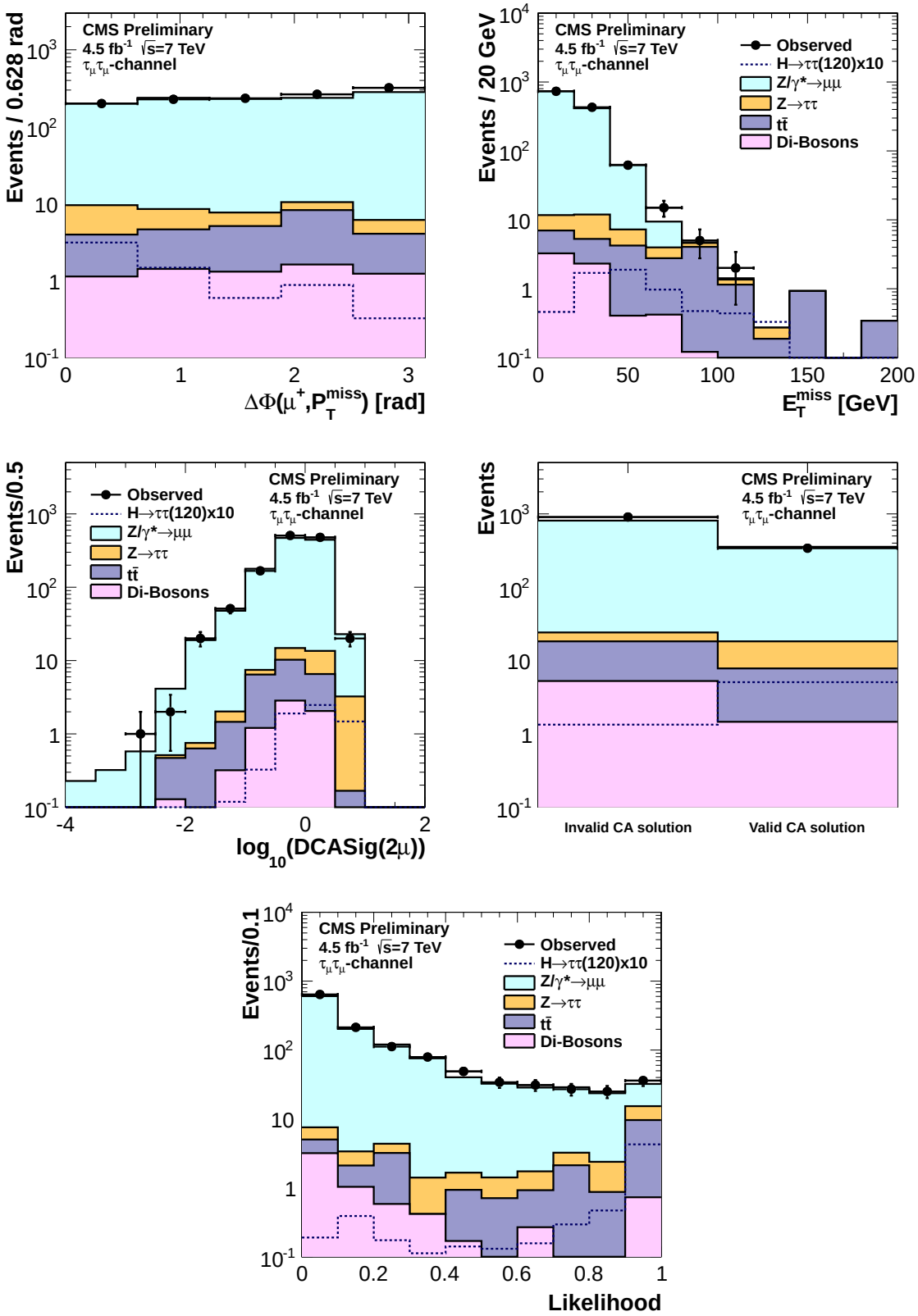

Figure 4: Distributions of discriminating variables in the *VBF* event category for the SM Higgs boson search. See text for the definition of the variables. 2011 data, represented by circles, are compared with MC background samples, displayed as filled histograms. The SM Higgs boson signal expected for $m_H = 120$ GeV/c^2, scaled to the SM cross section and multiplied by a factor of 10, is shown as dashed histograms.

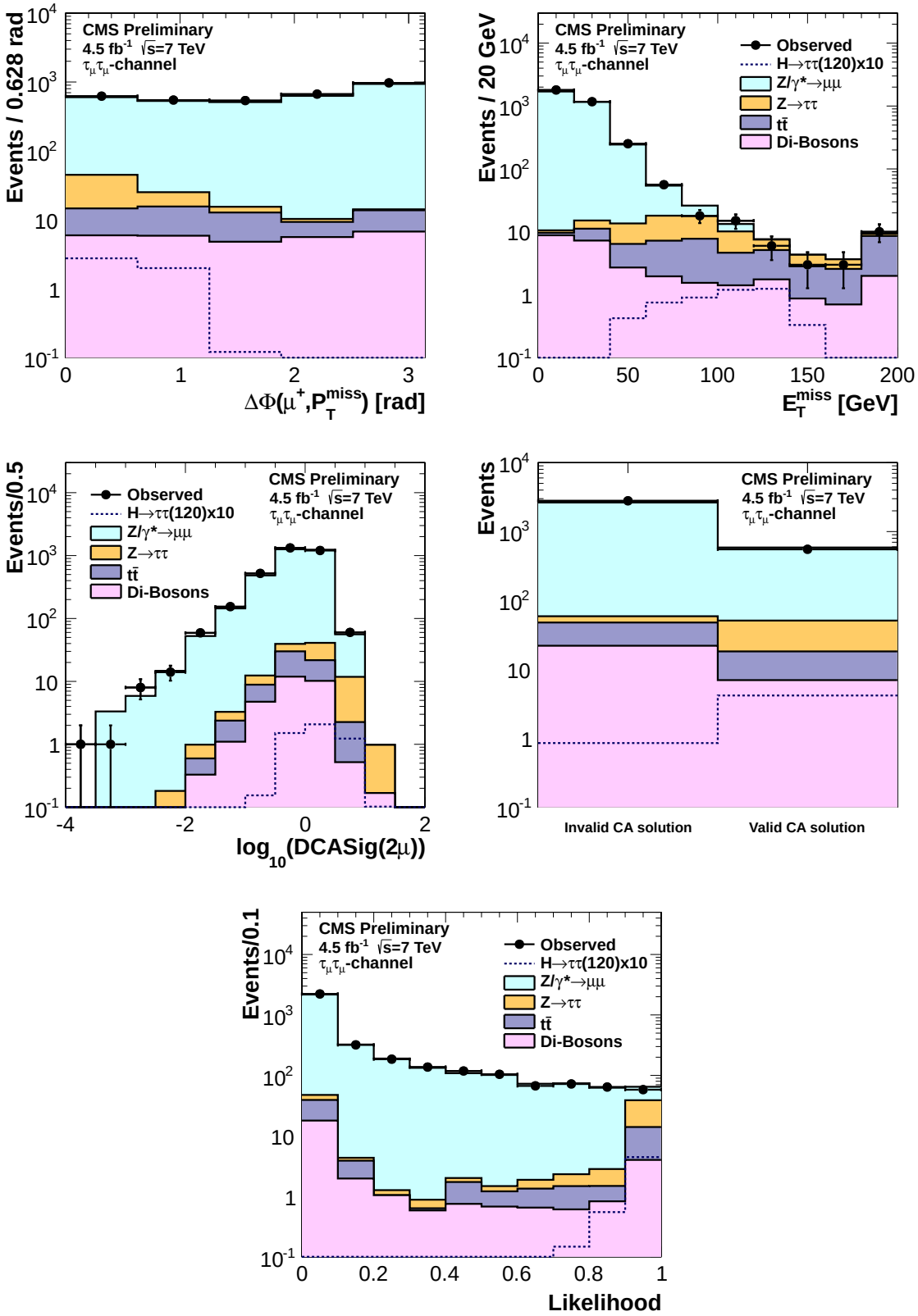

Figure 5: Distributions of discriminating variables in the *Boosted* event category for the SM Higgs boson search. See text for the definition of the variables. 2011 data, represented by circles, are compared with MC background samples, displayed as filled histograms. The SM Higgs boson signal for $m_H = 120$ GeV/c^2, scaled to the SM cross section and multiplied by a factor of 10, is shown as dashed histogram.

4 Background Sources

The events selected by the requirements described in Section 3 predominantly stem from Z decays into pairs of muons, or pairs of taus that subsequently decay into muons. The di-muon Drell-Yan background is evaluated directly from data by exploiting the difference in the shapes of the DCA significance of the two muons between the $Z/\gamma^* \to \mu\mu$ and $Z(H/\phi) \to \tau\tau \to 2\mu 4\nu$ events. The measurement is performed for different ranges of the reconstructed invariant mass of a muon-pair.

The contribution from $Z \to \tau\tau$ decays is estimated using a sample of $Z/\gamma^* \to \mu\mu$ events in which the muons are replaced ("embedded") with simulated decays of tau-leptons to muons. As a consequence, the kinematic properties of the tau-leptons used for this process are inherently correct due to the principle of lepton universality. For the selection of these $Z/\gamma^* \to \mu\mu$ events, the same criteria as in the Higgs boson search are used for the trigger, transverse momentum and pseudorapidity. Both muons are required to be isolated and their invariant mass has to exceed 50 GeV/c^2. This approach models correctly the Z boson recoil as well as the underlying event and contributions from pile-up events. The normalization of the $Z \to \tau\tau$ background is performed by matching the numbers of events in the embedded sample and a regular MC sample scaled to the cross section of inclusive Z boson production measured by CMS [26].

Another significant source of background comes from top-quark pair production, which is estimated using samples of simulated events. The normalization of this background contribution is controlled in the large $\not{E}_T > 80$ GeV region, which is almost entirely populated by top-quark pair production.

The QCD multijet background is estimated using ratios of same-sign (SS) and opposite-sign (OS) events. The isolation requirement is inverted for both muons to enhance the QCD multijet contribution. The mass shape of the SS events is used as the background template in the OS signal region.

Background contributions from di-boson production (WW, WZ and ZZ) and single W production are estimated using samples of simulated events. The yields of di-boson production are scaled to cross sections predicted by theory in NLO [27, 28], whereas the contribution from single W production is normalized to the inclusive cross section as measured by CMS [26].

The observed and expected numbers of events in each category of the SM and MSSM searches are reported in Table 2. The simulated numbers of events are given for a representatively chosen Higgs boson mass hypothesis $m_H = 120$ GeV/c^2 in the SM search and $m_A = 200$ GeV/c^2 in the MSSM search and are listed together with the estimated uncertainties on their yields.

5 Signal Extraction

The statistical analysis of a possible Higgs boson signal is based on a binned likelihood function, which is constructed from the two-dimensional distribution $\mathcal{D}(m_{\mu\mu}, m_{\tau\tau})$ in order to discriminate signal against $Z/\gamma^* \to \mu\mu$ and $Z \to \tau\tau$ backgrounds at the same time. The discrimination power is significantly weaker when only a single variable, $m_{\mu\mu}$ or $m_{\tau\tau}$, is used. In the case of the *Non B-Tag* category of the MSSM search, the two-dimensional distribution $\mathcal{D}(\not{E}_T, m_{\tau\tau})$ is used for the statistical inference when testing Higgs boson masses $m_A \geq 250$ GeV/c^2. This approach yields higher sensitivity to a MSSM Higgs signal at $m_A \geq 250$ GeV/c^2 compared to $\mathcal{D}(m_{\mu\mu}, m_{\tau\tau})$. Bins with zero signal expectations are removed from the likelihood function.

Table 2: Number of expected and observed events in the event categories as described in the text, after applying the requirement on the likelihood discriminant.

	Standard Model			MSSM	
Category	*0/1-Jet*	*Boosted*	*VBF*	*Non B-Tag*	*B-Tag*
$Z/\gamma^* \to \mu\mu$	118100 ± 6900	26.0 ± 5.8	16.9 ± 4.0	31030 ± 1510	3980 ± 255
$Z/\gamma^* \to \tau\tau$	3035 ± 182	24.8 ± 1.7	5.7 ± 0.6	1096 ± 66	55.5 ± 3.5
$t\bar{t}$	220 ± 20	10.0 ± 2.0	8.9 ± 2.0	36.1 ± 5.0	220 ± 25
QCD multijet	156 ± 17	-	-	74 ± 12	1.8 ± 1.8
W+jets	30 ± 9	-	-	22.2 ± 7.4	-
Di-bosons	324 ± 100	4.0 ± 1.4	0.73 ± 0.26	137 ± 43	23.0 ± 6.8
Total Background	121900 ± 6900	64.8 ± 6.7	32.2 ± 4.5	32395 ± 1512	4280 ± 256
Data	119905	58	36	31772	4340

The tau-pair mass, $m_{\tau\tau}$, is reconstructed using an algorithm that estimates the original tau three-momenta by maximizing a likelihood function with respect to free parameters corresponding to the missing tau-neutrino momenta, and which is subject to all applicable kinematic constraints [9]. Other terms in the likelihood take into account the tau-decay phase space and the probability density in the tau transverse momentum, parametrized as a function of $m_{\tau\tau}$. This algorithm yields a $m_{\tau\tau}$ distribution with a mean consistent with the true value, and with a nearly Gaussian shape. The relative mass resolution is ∼24% at a Higgs boson mass of 130 GeV/c^2, to be compared with ∼30% for the (non-Gaussian) distribution of the invariant mass reconstructed from the visible tau-decay products, $m_{\mu\mu}$.

The spectra of $m_{\tau\tau}$ and $m_{\mu\mu}$ are shown in Figures 6-10 for the previously defined event categories. The CMS data are compared to the samples of simulated events. The latter account for all expected background contributions and the prediction for a Higgs boson signal as expected for a $m_A = 200\,\text{GeV}/c^2$ and $\tan\beta = 20$ hypothesis for the MSSM event categories, and for a mass hypothesis of $m_H = 120\,\text{GeV}/c^2$ for the SM event categories.

The expected signal and background yields and the data yields, for the $(m_{\mu\mu}, m_{\tau\tau})$ bins in which non-zero signal events are expected, are shown in Tables 3 and 4 for the event categories of the SM search and in Table 5 for the event categories of the MSSM search.

Table 3: Expected signal (S), background (B) and data (Data) yields for the SM Higgs boson search, for the *Boosted* and the *VBF* event categories. The expected signal yields are given for a mass hypothesis of $m_H = 120$ GeV/c^2 and are scaled by a factor of 10. The yields are given in a two-dimensional $(m_{\mu\mu}[\text{GeV/c}^2], m_{\tau\tau}[\text{GeV/c}^2])$ binning.

VBF					*Boosted*				
$m_{\mu\mu}$	$m_{\tau\tau}$	S×10	B	Data	$m_{\mu\mu}$	$m_{\tau\tau}$	S×10	B	Data
$0-75$	$0-100$	0.26	4.11	4	$0-80$	$0-105$	1.24	23.7	21
$0-75$	$100-120$	1.84	1.04	0	$0-80$	$105-125$	1.76	8.12	4
$0-75$	$120-150$	2.13	1.88	5	$0-80$	$125-150$	1.71	2.13	1
$75-105$	$100-120$	0.06	2.69	4	$0-80$	$150-200$	0.07	1.08	2
$75-105$	$120-150$	0.05	4.89	1	$80-100$	$0-105$	0.05	1.81	0

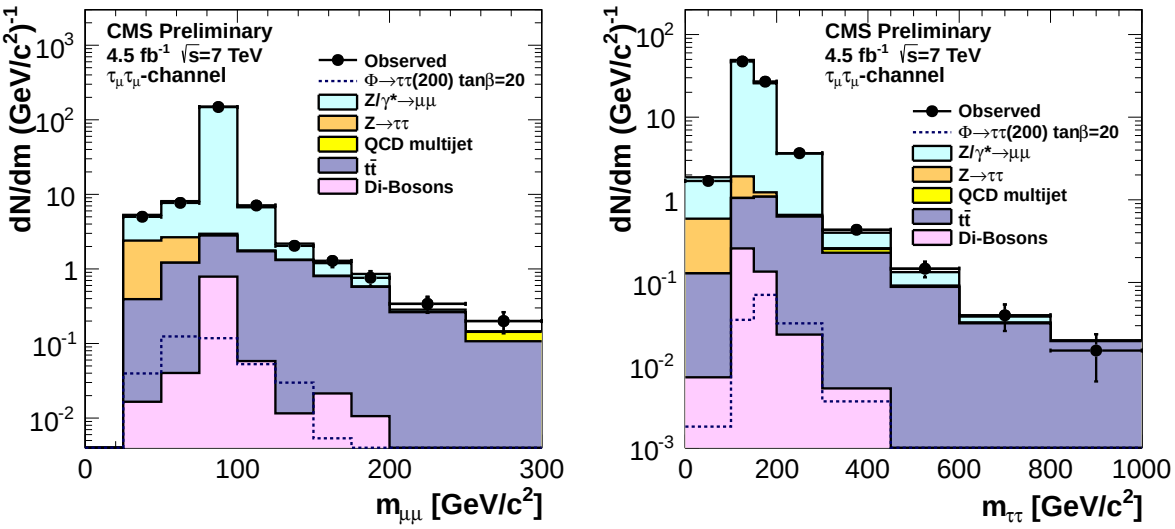

Figure 6: Distributions of the muon-pair invariant mass (left) and the tau-pair invariant mass (right) for events selected in the *B-Tag* category. CMS data, respresented by circles, are compared to the expectations from samples of simulated background events, displayed as filled histograms, and simulated MSSM signal events expected for $m_A = 200\,\mathrm{GeV}/c^2$ and $\tan\beta = 20$, shown as dashed histograms.

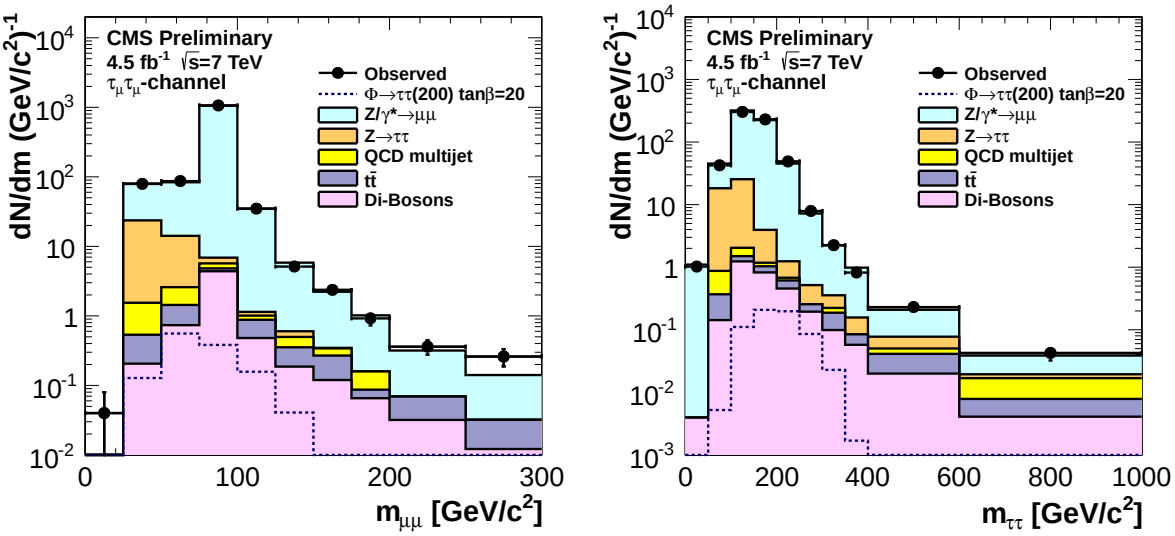

Figure 7: Distributions of the muon-pair invariant mass (left) and the tau-pair invariant mass (right) for events selected in the *Non B-Tag* category. CMS data, respresented by circles, are compared to the expectations from samples of simulated background events, displayed as filled histograms, and simulated MSSM signal events expected for $m_A = 200\,\mathrm{GeV}/c^2$ and $\tan\beta = 20$, shown as dashed histograms.

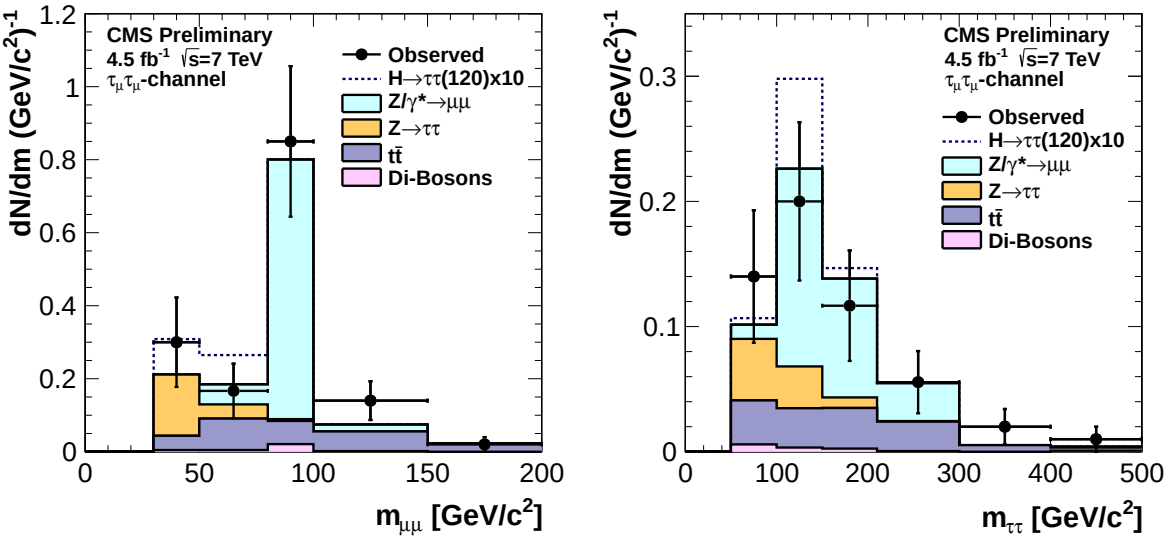

Figure 8: Distribution of the muon-pair mass (left) and tau-pair mass (right) for events selected in the sample of the *VBF* category. CMS data, respresented by circles, are compared to the expectations from samples of simulated background events, displayed as filled histograms. Simulated SM Higgs signal events expected for $m_H = 120\,\text{GeV}/c^2$, scaled to the SM cross section and multiplied by a factor of 10, are shown as dashed histograms.

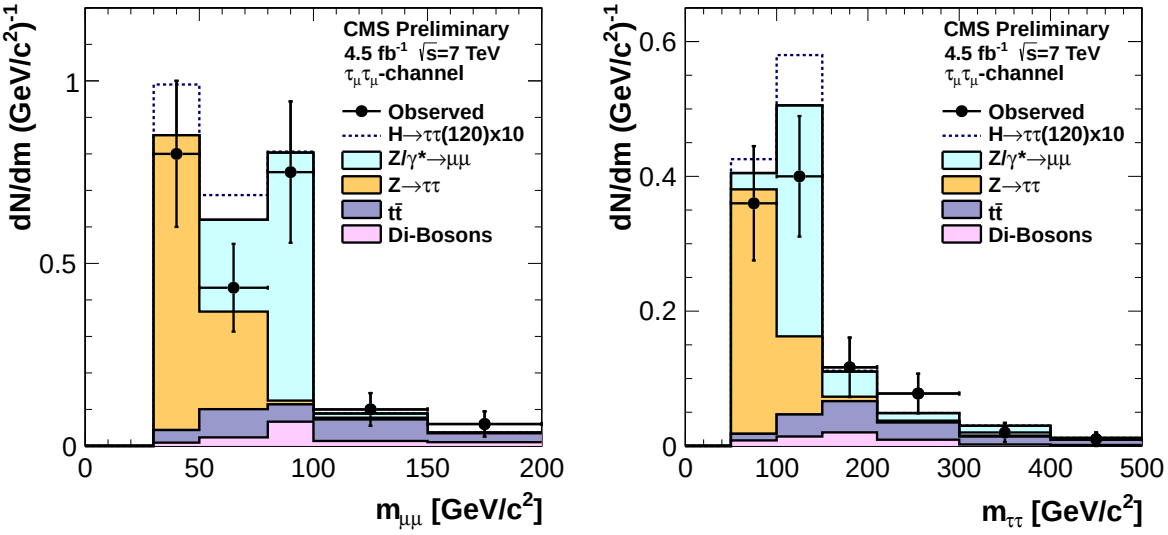

Figure 9: Distributions of the muon-pair mass (left) and tau-pair mass (right) for events selected in the sample of the *Boost* category. CMS data, respresented by circles, are compared to the expectations from samples of simulated background events, displayed as filled histograms. Simulated SM Higgs signal events expected for $m_H = 120\,\text{GeV}/c^2$, scaled to the SM cross section and multiplied by a factor of 10, are shown as dashed histograms.

Table 4: Expected signal (S), background (B) and data (Data) yields for the SM Higgs boson search, for the *0/1-Jet* event category. The expected signal yields are given for a mass hypothesis of $m_H = 120$ GeV/c^2 and are scaled by a factor of 10. The yields are given in a two-dimensional $(m_{\mu\mu}[\mathrm{GeV/c^2}], m_{\tau\tau}[\mathrm{GeV/c^2}])$ binning.

0/1-Jet				
$m_{\mu\mu}$	$m_{\tau\tau}$	S×10	B	Data
0 – 40	0 – 80	1.01	2188	2309
0 – 40	80 – 100	3.74	631	593
0 – 40	100 – 120	1.73	160	142
0 – 40	120 – 140	1.35	35.3	35
0 – 40	140 – 180	1.93	11.9	12
40 – 80	0 – 80	0.67	1399	1480
40 – 80	80 – 100	7.97	3301	3195
40 – 80	100 – 120	23.7	3859	3754
40 – 80	120 – 140	27.7	2792	2834
40 – 80	140 – 180	26.8	2680	2696
40 – 80	180 – 300	5.61	390	392
80 – 100	100 – 120	0.39	10010	9394
80 – 100	120 – 140	2.16	23111	22850
80 – 100	140 – 180	4.23	40732	40910
80 – 100	180 – 300	1.86	23959	24340
100 – 150	180 – 300	0.63	1951	1944

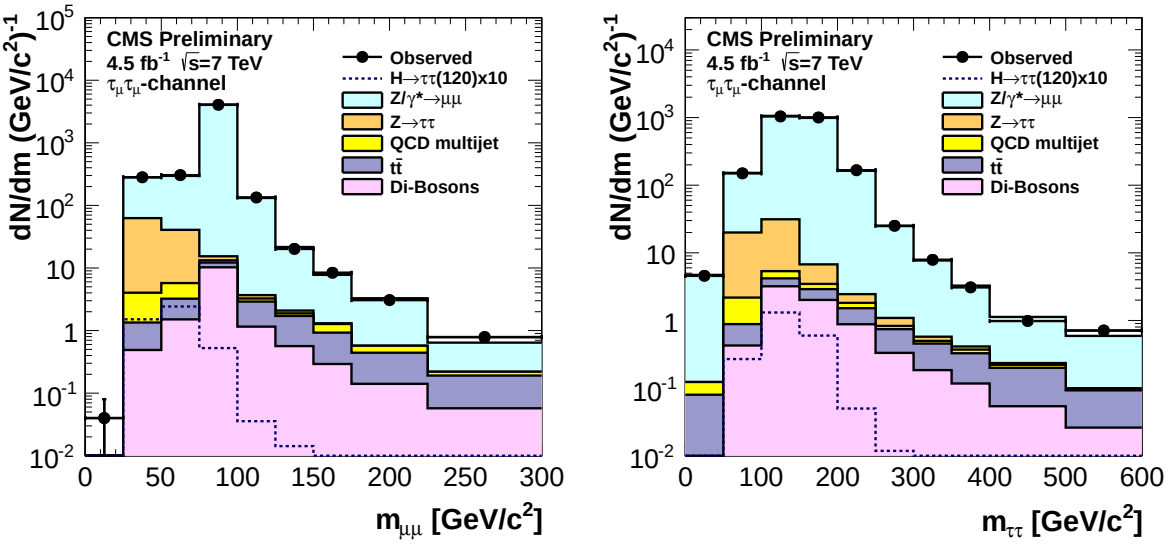

Figure 10: Distributions of the muon-pair mass (left) and tau-pair mass (right) for events selected in the sample of the *0/1-Jet* category. CMS data, respresented by circles, are compared to the expectations from samples of simulated background events, displayed as filled histograms. Simulated SM Higgs signal events expected for $m_H = 120\,\mathrm{GeV}/c^2$, scaled to the SM cross section and multiplied by a factor of 10, are shown as dashed histograms.

Table 5: Expected signal (S), background (B) and data (Data) yields for the MSSM Higgs boson search, for the *Non B-Tag* and the *BTag* event categories. The expected signal yields are given for a mass hypothesis of $m_A = 200$ GeV/c^2 and $\tan\beta = 20$. The yields are given in a two-dimensional ($m_{\mu\mu}$[GeV/c^2], $m_{\tau\tau}$[GeV/c^2]) binning.

Non B-Tag					*BTag*				
$m_{\mu\mu}$	$m_{\tau\tau}$	S	B	Data	$m_{\mu\mu}$	$m_{\tau\tau}$	S	B	Data
20 − 40	0 − 100	0.11	737	738	30 − 60	0 − 100	0.18	127.9	126
20 − 40	100 − 140	0.27	68.2	67	30 − 60	100 − 150	0.83	44.1	35
20 − 40	140 − 180	0.06	3.76	4	30 − 60	150 − 180	0.59	4.08	3
40 − 60	0 − 100	0.15	1176	1178	30 − 60	180 − 250	0.80	4.02	7
40 − 60	100 − 140	2.24	760	780	60 − 80	100 − 150	0.80	131.2	147
40 − 60	140 − 180	2.38	94.5	93	60 − 80	150 − 180	0.84	25.9	24
40 − 60	180 − 220	1.44	15.2	13	60 − 80	180 − 250	0.61	9.45	15
40 − 60	220 − 260	0.11	4.00	2	60 − 80	250 − 400	0.07	4.26	5
40 − 60	260 − 600	0.17	3.53	5	80 − 100	100 − 150	0.14	2151	2125
60 − 70	100 − 140	0.72	412	392	80 − 100	150 − 180	0.77	814	848
60 − 70	140 − 180	2.61	117	137	80 − 100	180 − 250	1.26	556	573
60 − 70	180 − 220	2.44	14.9	16	80 − 100	250 − 400	0.12	48.9	58
60 − 70	220 − 260	1.38	6.24	4	100 − 130	150 − 180	0.12	49.8	54
70 − 80	100 − 140	0.33	760	717	100 − 130	180 − 250	0.90	58.7	56
70 − 80	140 − 180	1.64	442	470	100 − 130	250 − 400	0.42	17.2	25
70 − 80	180 − 220	1.57	66.0	71	130 − 160	180 − 250	0.21	28.8	24
70 − 80	220 − 260	1.67	16.9	11	130 − 160	250 − 400	0.48	11.9	12
70 − 80	260 − 600	0.55	5.83	5	160 − 200	250 − 400	0.08	15.6	20
80 − 100	100 − 140	0.11	10019	9511					
80 − 100	140 − 180	0.95	10287	10306					
80 − 100	180 − 220	2.61	4698	4752					
80 − 100	220 − 260	1.90	801	820					
80 − 100	260 − 600	1.30	282	302					
100 − 130	140 − 180	0.17	390	367					
100 − 130	180 − 220	1.18	249	247					
100 − 130	220 − 260	1.39	115	118					
100 − 130	260 − 600	1.53	58.7	56					
130 − 180	180 − 220	0.08	62.0	47					
130 − 180	220 − 260	0.21	40.9	42					
130 − 180	260 − 600	0.43	47.3	51					
180 − 220	260 − 600	0.09	22.6	20					

6 Systematic Uncertainties

Systematic uncertainties on the yields are represented by nuisance parameters in the likelihood function for the $m_{\mu\mu}$, $m_{\tau\tau}$ and $\not\!\!E_T$ spectra, assuming a log normal prior for parameters that affect normalization, and Gaussian prior for parameters that affect the shape of the mass spectrum. The sources of uncertainties and their effect on event yields in the event categories of the SM and MSSM searches are summarized in Table 6.

The main sources of normalization uncertainties include the integrated luminosity (4.5%) [29], the jet energy scale (2-5% depending on jet transverse momentum and pseudorapidity), as well as the muon trigger and selection efficiencies (2.0%). The efficiency to identify a jet as b-tagged carries an uncertainty of 10%, and the b mistag rate is uncertain to 30% [30].

The normalization of the $Z/\gamma^* \to \mu\mu$ background is measured to a precision of 4-6%, depending on the reconstructed invariant mass of a muon-pair. Additionally, statistical uncertainties of 3-5% are assigned to the yields of $Z/\gamma^* \to \mu\mu$ events selected in the low statistics event categories of the SM search (*VBF* and *Boosted*) and MSSM search (*B-Tag*).

The contribution from the $Z \to \tau\tau$ background is estimated using the "embedded" event sample. The normalization of the embedded sample is scaled to the inclusive Z boson production cross section measured by CMS to a precision of 2.5% [26] and includes an additional uncertainty of 2% due to the non-linearity of the luminosity measurement [29]. The yields of $Z \to \tau\tau$ events are assigned an additional systematic uncertainties of 2.5-3% estimated by comparing the efficiency of the likelihood discrimination between the embedded sample and the regular MC simulation of $Z \to \tau\tau$ events. Lastly, an uncertainty between 0.5% and 8% is assigned to the estimated yields of $Z \to \tau\tau$ events selected in the different SM and MSSM event categories, due to the limited statistics of the embedded sample.

The normalization of the top-pair background is determined in the control region, $\not\!\!E_T > 80$ GeV, with an uncertainty of 8%.

The yields of di-boson events are scaled to the NLO cross sections as determined in [27, 28], with an uncertainty of 30%.

The uncertainties on the yields of single W events are found to have a negligible effect in the statistical analysis.

The limited statistical power of the simulated samples results in a statistical uncertainty up to 22% in the low statistics event categories of the SM and MSSM search, for the dominant $t\bar{t}$ and $Z/\gamma^* \to \mu\mu$ backgrounds and 10-100% for the simulated signal samples.

The $\not\!\!E_T$ scale in data relative to the simulated $\not\!\!E_T$ scale is extracted by template fitting the $\not\!\!E_T$ distribution. The templates are generated for the nominal value and with shifts of $\not\!\!E_T$ up to $\pm$10%, with steps of 1%. The procedure is performed separately for two classes of events: for $t\bar{t}$, fitting the region $\not\!\!E_T > 80$ GeV dominated by $t\bar{t}$ production, and for $Z/\gamma^* \to \mu\mu$, fitting the region $\not\!\!E_T < 80$ GeV dominated by $Z/\gamma^* \to \mu\mu$. The uncertainty on the $\not\!\!E_T$ scale ranges between 1% and 5% depending on the signal or background process and on the event category. For the *VBF* and *Boosted* event categories, the $\not\!\!E_T$ scale uncertainty affects the background and signal normalization as estimated with the samples of simulated events. Furthermore, $\not\!\!E_T$ is used for the reconstruction of $m_{\tau\tau}$ with the method described in Section 5 and alters the shape of the $m_{\tau\tau}$ distribution. The $\not\!\!E_T$ scale uncertainty is therefore represented by a nuisance parameter whose variation results in a continuous modification of the $m_{\tau\tau}$ spectrum shape [31]. The uncertainties associated with the muon-energy scale alter both the absolute normalization and the shapes of the mass spectra. Since the muon-energy scale is known to a precision better than 1%, it is

neglected in the statistical analysis.

The theoretical uncertainties of Higgs boson production cross section are included (12-25% for $gg \to H$, 4% for $qq \to qqH$, 10-15% for $gg \to \phi$ and 15-25% for $gg \to b\bar{b}\phi$) [32] in the statistical analysis of the SM and MSSM search.

The uncertainties associated with parton distribution functions (PDFs) and the strong coupling constant α_s translate into an uncertainty of 8% on the signal event yields. The uncertainties related to the simulation of the underlying event and parton showering result in an uncertainty of 4% on the signal event yields.

7 Results

The analysis finds no evidence for the presence of a Higgs boson signal. 95% confidence level (CL) upper limits are set, in the SM case, on the cross section of the Higgs boson production relative to the expected SM Higgs production cross section, and in the MSSM case on $\tan\beta$ as a function of the pseudoscalar Higgs boson mass m_A in the context of the MSSM m_h–max scenario. These limits are computed with the RooStats toolkit [33].

7.1 SM Limits

A 95% CL upper limit is set on the ratio of the probed cross section of the Higgs boson, $\sigma(pp \to H) \times \mathcal{B}(H \to \tau\tau)$ (denoted hereafter as $\sigma_H \times B_{\tau\tau}$), relative to the value predicted by the SM. For the limit setting, a frequentist inference is employed, where the CL_s criterion is applied and a profiled likelihood ratio is used as described in [34]. Figure 11 shows the observed and the median expected 95% CL upper limits for Higgs boson mass hypotheses ranging from 110 to 145 GeV/c^2. The bands represent the 68% and 95% probability intervals around the median expected limit. Table 7 lists both the expected and the observed limits for the different Higgs boson mass hypotheses. An upper limit on $\sigma_H \times B_{\tau\tau}$ is set in the range $7.7-34.7$ times the SM value.

7.2 MSSM Limits

In the *B-Tag* and *Non B-Tag* event categories, a 95% CL upper limit on $\tan\beta$ is set as a function of the pseudoscalar Higgs boson mass m_A. Signal contributions from h, H and A production are considered. The ratio between the gluon fusion process and production associated with b quarks, depend on the value of $\tan\beta$. To account for this, a scan of $\tan\beta$ is performed for each tested m_A hypothesis. The procedure is analog to the one used in Ref. [9]. Limits are computed with an asymptotic CL_s approach based on the profiled likelihood ratio [35].

Figure 12 shows the region in the parameter space of $\tan\beta$ versus m_A excluded at 95% CL in the context of the MSSM m_h–max scenario. The exclusion region obtained with experimental data is in agreement with the expection from background-only. Values of $\tan\beta$ larger than 16.9 (53.5) are excluded for m_A =90 GeV/c^2 (m_A =400 GeV/c^2). The values for the observed and expected upper limits are listed in Table 8.

Experimental Uncertainties		Propagated to Limit Calculation				
Uncertainty	Estimate	*0/1-Jet*	*Boosted*	*VBF*	*Non B-Tag*	*B-Tag*
normalization altering uncertainties						
Luminosity (Di-bosons, signal)	$\pm 4.5\%$	$\pm 4.5\%$	$\pm 4.5\%$	$\pm 4.5\%$	$\pm 4.5\%$	$\pm 4.5\%$
Muon ID & Trigger	$\pm 2\%$	$\pm 4\%$	$\pm 4\%$	$\pm 4\%$	$\pm 4\%$	$\pm 4\%$
JES	$\pm 2-5\%$	$\mp 1-6\%$	$\pm 4-6\%$	$\pm 10-20\%$	$\mp 2\%$	$\pm 5\%$
b-Tagging Efficiency	$\pm 10\%$	–	–	–	$\mp 1\%$	$\pm 5\%$
Mis-Tagging	$\pm 30\%$	–	–	–	$\pm 4\%$	$\mp 2\%$
Norm. $Z \to \tau\tau$	$\pm 3.3\%$	$\pm 3.3\%$	$\pm 3.3\%$	$\pm 3.3\%$	$\pm 3.3\%$	$\pm 3.3\%$
Likelihood selection ($Z \to \tau\tau$)		$\pm 3\%$	$\pm 2.5\%$	$\pm 2.5\%$	$\pm 3\%$	$\pm 3\%$
Statistics of the $Z \to \tau\tau$ embedded sample		$< 1\%$	$\pm 3.5\%$	$\pm 8\%$	$< 1\%$	$\pm 2-3.5\%$
Norm. $Z \to \mu\mu$	$\pm 4-6\%$	$\pm 4-6\%$	$\pm 4-6\%$	$\pm 4-6\%$	$\pm 4-6\%$	$\pm 4-6\%$
Scale factors for event categories (Relative stat. error) $Z \to \mu\mu$		$< 0.2\%$	$\pm 3\%$	$\pm 5\%$	$< 0.2\%$	$\pm 3\%$
Norm. $t\bar{t}$	$\pm 8\%$	$\pm 8\%$	$\pm 8\%$	$\pm 8\%$	$\pm 8\%$	$\pm 8\%$
Di-boson production cross section	$\pm 30\%$	$\pm 30\%$	$\pm 30\%$	$\pm 30\%$	$\pm 30\%$	$\pm 30\%$
MC statistics						
$qq \to qqH$		$\pm 8-10\%$	$\pm 20-23\%$	$\pm 8-10\%$	–	–
$gg \to H$		$\pm 6-8\%$	$\pm 20-30\%$	$\pm 50-100\%$	–	–
$qq \to t\bar{t}H/VH$		$\pm 3-7\%$	$\pm 8-14\%$	$\pm 30-100\%$	–	–
$gg \to b\bar{b}\phi$		–	–	–	$\pm 3-7\%$	$\pm 7-18\%$
$gg \to \phi$		–	–	–	$\pm 3-7\%$	$\pm 22-100\%$
$Z \to \mu\mu$		$< 1\%$	$\pm 20\%$	$\pm 22\%$	$< 1\%$	$\pm 1-2.5\%$
$t\bar{t}$		$\pm 4\%$	$\pm 17\%$	$\pm 19\%$	$\pm 5-9\%$	$\pm 4-7\%$
normalization and shape altering uncertainties						
$\not{E}_T$ scale	$\pm 1-5\%$	–	$\pm 4-9\%$	$\pm 3-7\%$	–	–

Theory Uncertainties		Propagated to Limit Calculation				
Uncertainty	Estimate	*0/1-Jet*	*Boosted*	*VBF*	*Non B-Tag*	*B-Tag*
$\mu_r/\mu_f(gg \to H)$		$\pm 12\%$	$\pm 25\%$	$\pm 12\%$	-	-
$\mu_r/\mu_f(qq \to qqH)$		$\pm 4\%$	$\pm 4\%$	$\pm 4\%$	-	-
$\mu_r/\mu_f(gg \to \phi)$		-	-	-	$\pm 10-15\%$	$\pm 10-15\%$
$\mu_r/\mu_f(gg \to b\bar{b}\phi)$		-	-	-	$\pm 15-25\%$	$\pm 15-25\%$
PDFs + α_s		$\pm 8\%$	$\pm 8\%$	$\pm 8\%$	$\pm 8\%$	$\pm 8\%$
Underlying event & Parton showering		$\mp 4\%$	$\pm 4\%$	$\pm 4\%$	$\mp 4\%$	$\pm 4\%$

Table 6: Uncertainties used for the statistical analysis.

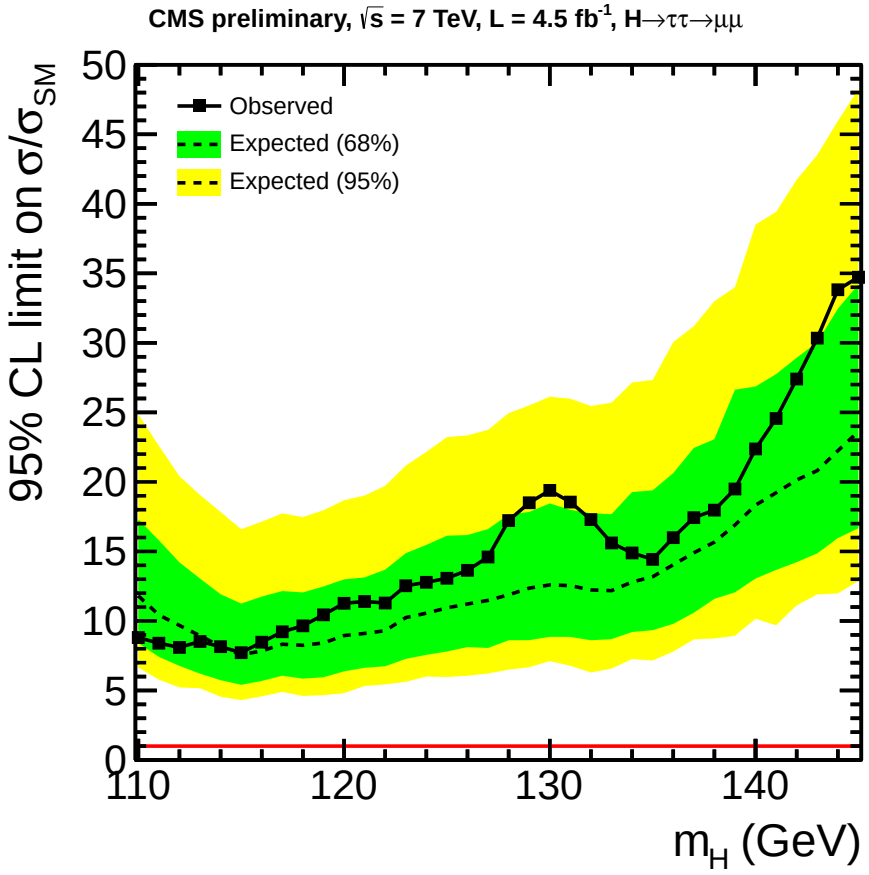

Figure 11: 95% C.L. upper limits on the ratio of the cross section of the Higgs boson, $\sigma(pp \rightarrow H) \times \mathcal{B}(H \rightarrow \tau\tau)$, relative to the value predicted by the SM as a function of the SM Higgs boson mass m_H. The observed limits (solid lines) are compared with the expected median limits (dashed lines). The green and yellow bands indicate the central 68% and 95% confidence level intervals for the observed limit, respectively.

Table 7: Expected range and observed 95% CL upper limits on the ratio of the cross section of the SM Higgs boson, $\sigma(pp \to H) \times \mathcal{B}(H \to \tau\tau)$, relative to the value predicted by the SM as a function of the Higgs boson mass m_H.

SM Higgs	Expected Limit [over σ(SM)]					
m_H [GeV/c^2]	-2σ	-1σ	Median	$+1\sigma$	$+2\sigma$	Obs. Limit
110	6.647	8.409	11.81	17.31	24.86	8.805
111	5.785	7.418	10.43	15.80	22.60	8.401
112	5.218	6.771	9.679	14.21	20.41	8.096
113	5.161	6.212	8.936	13.05	19.06	8.523
114	4.549	5.741	8.172	11.92	17.84	8.150
115	4.309	5.409	7.569	11.25	16.60	7.718
116	4.581	5.686	7.843	11.75	17.14	8.473
117	4.897	6.063	8.326	12.15	17.74	9.221
118	4.603	5.852	8.248	12.05	17.47	9.649
119	4.665	5.952	8.417	12.48	17.96	10.44
120	4.809	6.375	8.948	12.99	18.68	11.27
121	5.327	6.633	9.102	13.13	19.02	11.40
122	5.435	6.743	9.299	13.69	19.72	11.29
123	5.624	7.273	10.24	14.87	21.17	12.53
124	6.004	7.562	10.56	15.47	22.16	12.78
125	5.970	7.805	10.94	16.13	23.22	13.07
126	6.058	8.122	11.22	16.18	23.35	13.64
127	6.223	8.058	11.48	16.61	23.74	14.60
128	6.498	8.609	11.88	17.65	24.95	17.22
129	6.674	8.619	12.36	17.84	25.50	18.50
130	7.111	8.860	12.59	18.45	26.13	19.39
131	6.775	8.853	12.54	17.99	25.98	18.55
132	6.295	8.611	12.23	17.74	25.46	17.29
133	6.577	8.694	12.18	17.68	25.70	15.61
134	7.262	9.205	12.80	19.27	27.15	14.89
135	7.159	9.336	13.18	19.39	27.33	14.43
136	7.797	9.793	14.04	20.63	30.05	15.99
137	8.676	10.59	14.90	22.44	31.20	17.43
138	8.741	11.59	15.67	23.07	33.00	17.97
139	8.932	12.06	16.90	26.63	34.00	19.49
140	10.16	13.05	18.33	26.86	38.51	22.37
141	9.691	13.67	19.22	27.75	39.42	24.56
142	11.12	14.23	20.14	28.93	41.73	27.40
143	11.91	14.86	20.81	30.03	43.52	30.34
144	11.98	15.96	22.24	32.45	45.95	33.82
145	12.87	16.67	23.63	34.20	48.26	34.72

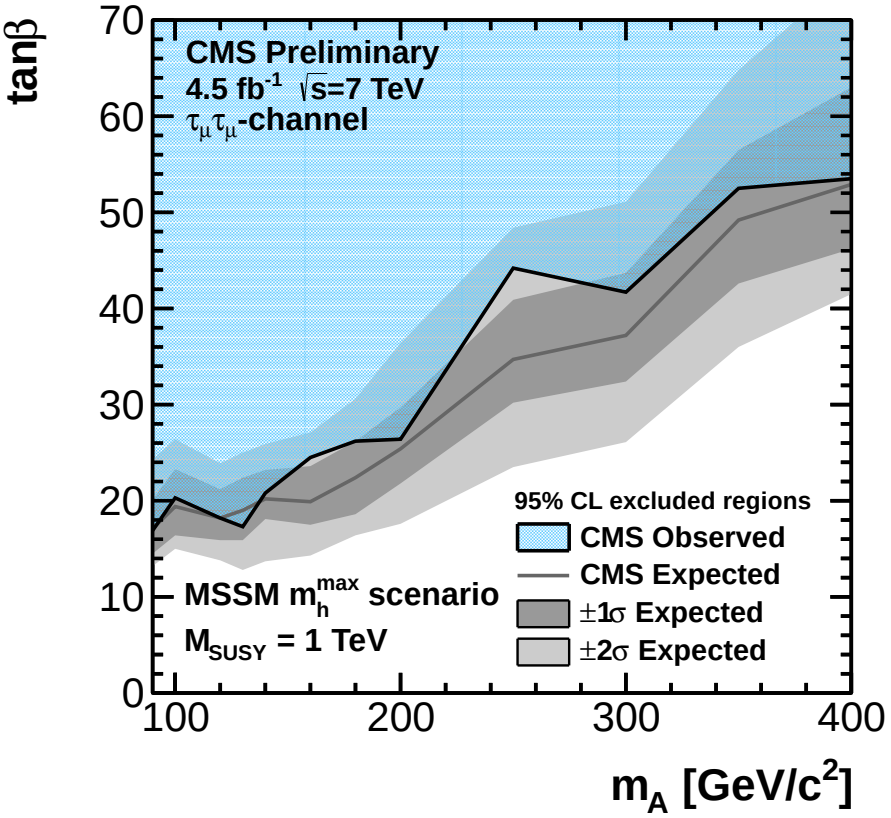

Figure 12: Region in the parameter space of $\tan\beta$ versus m_A excluded at 95% CL in the context of the MSSM m_h- max scenario. The expected one- and two-standard-deviation ranges and the observed 95% CL upper limits are shown together with the observed excluded region.

Table 8: Expected and observed 95% CL upper limits for $\tan\beta$ in the m_h- max scenario as functions of m_A, for the MSSM search.

MSSM Higgs	Expected Limit on $\tan\beta$					
m_A [GeV/c^2]	-2σ	-1σ	Median	$+1\sigma$	$+2\sigma$	Obs. Limit
90	13.2	14.5	17.1	20.1	24.3	16.9
100	15.0	16.4	19.4	23.3	26.4	20.3
120	13.8	15.9	18.2	21.2	23.9	18.2
130	12.8	15.9	19.0	22.4	25.0	17.3
140	13.7	18.1	20.2	23.2	25.9	20.8
160	14.3	17.5	19.9	23.6	27.1	24.5
180	16.4	18.6	22.4	26.2	30.6	26.2
200	17.6	21.8	25.4	29.7	36.4	26.4
250	23.5	30.2	34.7	40.9	48.4	44.2
300	26.1	32.4	37.2	43.7	51.1	41.7
350	36.0	42.6	49.2	56.5	64.8	52.5
400	41.5	46.2	52.9	63.0	-	53.5

8 Summary

A search for neutral Higgs bosons decaying into tau-pairs is performed in the di-muon and $\not\!\!E_{\mathrm{T}}$ channel, which is characterized by a large Drell-Yan background and a small branching fraction. Neutral Higgs bosons are expected both in the context of the Standard Model (SM) as well as in its Minimal Supersymmetric extension (MSSM). Regarding the SM case, three Higgs boson production mechanisms are addressed: gluon fusion, vector boson fusion and the production of a highly boosted Higgs boson. For the MSSM Higgs boson search, two production mechanisms are studied: gluon fusion and b quark associated production. The signal fraction in each event category is enhanced by a multi-variate analysis combining orthogonal kinematic variables into a likelihood discriminant. Two-dimensional distributions of either the reconstructed mass of muon-pair versus the reconstructed mass of the tau-pair system or the missing transverse energy versus the reconstructed tau-pair invariant mass are constructed to examine the data for the presence of a Higgs signal. No significant excess over the expectation from the expected SM background contributions is observed. The results of the analysis are presented as upper limits on the Higgs boson production cross sections (SM), or as upper limits on the range of $\tan\beta$ (MSSM). In case of the SM, an upper limit on $\sigma(pp \to H) \times \mathcal{B}(H \to \tau\tau)$ is set in the range 7.7 - 34.7 times the value of the SM cross section. For the MSSM, the upper bound on $\tan\beta$ ranges from 16.9 to 53.5.

References

[1] F. Englert and R. Brout, "Broken symmetry and the mass of gauge vector mesons", *Phys. Rev. Lett.* **13** (1964) 321. doi:10.1103/PhysRevLett.13.321.

[2] P. W. Higgs, "Broken symmetries, massless particles and gauge fields", *Phys. Lett.* **12** (1964) 132. doi:10.1016/0031-9163(64)91136-9.

[3] P. W. Higgs, "Broken symmetries and the masses of gauge bosons", *Phys. Rev. Lett.* **13** (1964) 508. doi:10.1103/PhysRevLett.13.508.

[4] G. S. Guralnik, C. R. Hagen, and T. W. B. Kibble, "Global conservation laws and massless particles", *Phys. Rev. Lett.* **13** (1964) 585. doi:10.1103/PhysRevLett.13.585.

[5] P. W. Higgs, "Spontaneous symmetry breakdown without massless bosons", *Phys. Rev.* **145** (1966) 1156. doi:10.1103/PhysRev.145.1156.

[6] T. W. B. Kibble, "Symmetry breaking in non-Abelian gauge theories", *Phys. Rev.* **155** (1967) 1554. doi:10.1103/PhysRev.155.1554.

[7] E. Witten, "Mass Hierarchies in Supersymmetric Theories", *Phys. Lett. B* **105** (1981) 267. doi:10.1016/0370-2693(81)90885-6.

[8] S. P. Martin, "A Supersymmetry Primer", (1997). arXiv:hep-ph/9709356. See also references therein.

[9] CMS Collaboration, "Search for Neutral Higgs Bosons Decaying to Tau Pairs in pp Collisions at $\sqrt{s}$ = 7 TeV", *to appear in Phys. Lett. B* (2012) arXiv:1202.4083.

[10] ATLAS Collaboration, "Search for neutral MSSM Higgs Bosons Decaying to $\tau^+\tau^-$ Pairs in Proton-Proton Collisions at $\sqrt{s}$ = 7 TeV with the ATLAS Experiment", **ATLAS-CONF-2011-024** (2011).

[11] CDF and D0 Collaboration, "Combined CDF and D0 Upper Limits on MSSM Higgs Boson Production in Tau-Tau Final States with up to 2.2 fb^{-1}", arXiv:1003.3363.

[12] LEP Higgs Working Group, "Search for Neutral MSSM Higgs Bosons at LEP", *Eur. Phys. J.* **C47** (2006) 547–587. doi:10.1140/epjc/s2006-02569-7.

[13] CMS Collaboration, "The CMS Experiment at the CERN LHC", *JINST* **0803** (2008) S08004. doi:10.1088/1748-0221/3/08/S08004.

[14] T. Sjöstrand, S. Mrenna, and P. Skands, "PYTHIA 6.4 Physics and Manual", *JHEP* **0605** (2006) 026. doi:10.1088/1126-6708/2006/05/026.

[15] S. Frixione, P. Nason, and C. Oleari, "Matching NLO QCD Computations with Parton Shower Simulations: the POWHEG Method", *JHEP* **0711** (2007) 070. doi:10.1088/1126-6708/2007/11/070.

[16] Z. Wąs et al., "TAUOLA the Library for Tau Lepton Decay", *Nucl. Phys. B, Proc. Suppl.* **98** (2001) 96. doi:10.1016/S0920-5632(01)01200-2.

[17] C. Anastasiou, K. Melnikov, and F. Petriello, "Fully differential Higgs boson production and the di-photon signal through next-to-next-to-leading order", *Nucl. Phys.* **B724** (2005) 197–246. doi:10.1016/j.nuclphysb.2005.06.036.

[18] C. Anastasiou, S. Bucherer, and Z. Kunszt, "HPro: A NLO Monte-Carlo for Higgs production via gluon fusion with finite heavy quark masses", *JHEP* **10** (2009) 068. doi:10.1088/1126-6708/2009/10/068.

[19] CMS Collaboration, "Performance of muon identification in pp collisions at $\sqrt{s}$ = 7 TeV", *CMS Physics Analysis Summary* **CMS-PAS-MUO-10-002** (2010).

[20] CMS Collaboration, "Particle–Flow Event Reconstruction in CMS and Performance for Jets, Taus, and $E_{\mathrm{T}}^{\mathrm{miss}}$", *CMS Physics Analysis Summary* **CMS-PAS-PFT-09-001** (2009).

[21] CMS Collaboration, "Commissioning of the Particle-Flow Reconstruction in Minimum-Bias and Jet Events from pp Collisions at 7 TeV", *CMS Physics Analysis Summary* **CMS-PAS-PFT-10-002** (2010).

[22] M. Cacciari, G. P. Salam, and G. Soyez, "The anti-k_T jet clustering algorithm", *JHEP* **04** (2008) 063. doi:10.1088/1126-6708/2008/04/063.

[23] CMS Collaboration, "Commissioning of b-jet identification with pp collisions at $\sqrt{s}$ = 7 TeV", *CMS Physics Analysis Summary* **CMS-PAS-BTV-10-001** (2010).

[24] OPAL Collaboration, "Search for the standard model higgs boson in e^+e^- collisions at $\sqrt{s}$ = 161 GeV - 172 GeV", *Eur. Phys. J.* **C1** (1998) 425–438. doi:10.1007/s100520050094.

[25] D. L. Rainwater, D. Zeppenfeld, and K. Hagiwara, "Searching for H to tau tau in weak boson fusion at the CERN LHC", *Phys.Rev.* **D59** (1998) 014037, arXiv:hep-ph/9808468. doi:10.1103/PhysRevD.59.014037.

[26] CMS Collaboration, "Measurement of Inclusive W and Z Cross Sections in pp Collisions $\sqrt{s}$=7 TeV", *JHEP* **1101** (2011) 080. doi:10.1007/JHEP01(2011)080.

[27] K. Melnikov and F. Petriello, "Electroweak gauge boson production at hadron colliders through $\mathcal{O}(\alpha_s^2)$", *Phys. Rev.* **D74** (2006) 114017, arXiv:hep-ph/0609070. doi:10.1103/PhysRevD.74.114017.

[28] K. Melnikov and F. Petriello, "The W boson production cross section at the LHC through $\mathcal{O}(\alpha_s^2)$", *Phys. Rev. Lett.* **96** (2006) 231803, arXiv:hep-ph/0603182. doi:10.1103/PhysRevLett.96.231803.

[29] CMS Collaboration, "Measurement of CMS Luminosity", *CMS Physics Analysis Summary* **EWK-10-004** (2010).

[30] CMS Collaboration, "Performance of b-jet identification in CMS", *CMS Physics Analysis Summary* **CMS-PAS-BTV-11-001** (2011).

[31] J. S. Conway, "Nuisance Parameters in Likelihoods for Multisource Spectra", *Proceedings of PhyStat 2011, CERN-2011-006* (2011) arXiv:1103.0354.

[32] LHC Higgs Cross Section Working Group, S. Dittmaier, C. Mariotti et al., "Handbook of LHC Higgs Cross Sections: 1. Inclusive Observables", *CERN-2011-002* (2011) arXiv:1101.0593.

[33] L. Moneta et al., "The RooStats Project", *PoS* **ACAT2010** (2010) 057, arXiv:1009.1003.

[34] The ATLAS collaboration, The CMS Collaboration and The LHC Higgs Combination Group, "Procedure for the LHC Higgs boson search combination in Summer 2011", *ATL-PHYS-PUB-2011-11, CMS NOTE-2011/005* (2011).

[35] G. Cowan, K. Cranmer, E. Gross and O. Vitells, "Asymptotic formulae for likelihood-based tests of new physics", *The European Physical Journal C - Particles and Fields* **71** (2011) 1–19. doi:10.1140/epjc/s10052-011-1554-0.